Airborne, direct-detection, 2-μm triple-pulse IPDA lidar for simultaneous and independent atmospheric water vapor and carbon dioxide active remote sensing

Tamer F. Refaat[a], Mulugeta Petros[a], Upendra N. Singh[a], Charles W. Antill[a], Teh-Hwa Wong[b], Ruben G. Remus[a], Karl Reithmaier[b], Jane Lee[b], Stephen C. Bowen[a], Bryant D. Taylor[c], Angela M. Welters[a], Anna Noe[a], and Syed Ismail[c]

[a]NASA Langley Research Center, Hampton, VA USA 23681

[b]Science Systems and Applications, Inc., Hampton, VA, USA 23666

[c]Analytical Services and Materials, Inc., Hampton, VA, USA 23666

ABSTRACT

Atmospheric water vapor and carbon dioxide are important greenhouse gases that significantly contribute to the global radiation budget on Earth. A 2-micron triple-pulse, Integrated Path Differential Absorption (IPDA) lidar instrument for ground and airborne atmospheric carbon dioxide and water vapor concentration measurements using direct detection was developed at NASA Langley Research Center. This active remote sensing instrument provides an alternate approach with significant advantages for measuring atmospheric concentrations of the gases. A high energy pulsed laser transmitter approach coupled with sensitive receiver detection provides a high-precision measurement capability by having a high signal-to-noise ratio. This paper presents the concept, development, integration and testing of the 2-micron triple-pulse IPDA. The integration includes the various IPDA transmitter, receiver and data acquisition subsystems and components. Ground and airborne testing indicated successful operation of the IPDA lidar.

Keywords: Triple-pulse laser, IPDA lidar, Carbon dioxide, Water vapor, Pulse detection

1. INTRODUCTION

Knowledge of the spatial and temporal distributions of atmospheric carbon dioxide (CO_2) in global and regional scales are critical for predicting and understanding the radiation budget and carbon cycle processes and possibly managing global warming. Estimating sources and sinks, and transport of CO_2 has become the topic of vital importance to the scientific community. In response to these challenging objectives, NASA has been conducting elaborate carbon studies using a myriad of instruments based on ground, airborne and space platforms. Several differential absorption lidar (DIAL) systems have been developed at NASA Langley Research Center (LaRC) for active remote sensing of CO_2 [1-11]. These instruments are based on pulsed 2-μm transmitter technologies, which also provide direct range and aerosol measurements. Active remote sensing have a number of advantages, over passive remote sensing, during night, over seasons, at high latitudes, and over tropical ecosystem measurements. The 2-μm region offers attractive spectroscopic features that include strong CO_2 absorption, low temperature dependence and low interference from other atmospheric gases. In addition, for Integrated Path Differential Absorption (IPDA) lidar application, the 2-μm provides optimum low tropospheric weighting functions to focus on CO_2 near-surface dynamics [10-11].

For more than 20 years, researchers at LaRC have developed several high-energy and high repetition rate 2-μm pulsed lasers and other critical components for CO_2 DIAL applications [12]. These lasers adopt wavelength control schemes to precisely tune and lock the operating wavelength at any desired offset from a CO_2 line center reference [3, 13]. Range-resolved, aerosol backscatter CO_2 DIAL measurements, using single-pulse 2-μm transmitters, have been demonstrated by LaRC using coherent and direct detection techniques [1-3]. In the earlier developments, the wavelength of the transmitted pulses alternates between on-line and off-line positions at a relatively low rate (5-10 Hz). Wind and aerosols measurements are byproducts of the same lidar systems. These provided useful additional information on atmospheric structure coupled with CO_2 measurements. Detection technology usually limits the CO_2 DIAL profiling capability at the 2-μm wavelength. Therefore, in earlier 2-μm, direct detection, CO_2 DIAL systems developed at LaRC, phototransistors have been developed and integrated for the first time in lidar applications [1-2]. These results demonstrated the capabilities of the DIAL system in profiling atmospheric CO_2 using the 2-μm wavelength for both range resolved and integrated column content measurements.

Upgrading the 2-μm laser technology, double-pulse lasers have been demonstrated with energy as high as 600 mJ and up to 10 Hz repetition rate [12, 14]. The two laser pulses, separated by 200 μs, are generated using a single pump pulse and can be tuned and locked separately. Using this transmitter, NASA LaRC developed and demonstrated the double-pulsed 2-μm direct detection IPDA lidar for CO_2 column measurement from an airborne platform. This double-pulse IPDA was tuned with respect to the CO_2 R30 strong absorption line. Airborne field experiments were conducted to quantify and characterize instrument capabilities, sensitivity and bias errors by comparison to performance models. Double-pulse IPDA range measurements from ground indicated a 0.93 m uncertainty. CO_2 IPDA differential optical depth measurements agree with models. For example, CO_2 differential optical depth measurements over ocean from 3.1 and 6.1 km altitudes indicated 0.95% and 0.83% uncertainty, respectively, using 10 second (100 shots) averaging. Using the same averaging 0.40% uncertainty was observed over land, from 3.4 km altitude, due to higher surface reflectivity, which increases the return signal power and enhances the signal-to-noise ratio. However, less uncertainty is observed at higher altitudes due to reduced signal shot noise, indicating that detection system noise-equivalent-power dominates the error. These results show that the IPDA technique is well suited for high altitude operation such as space-based platforms [10]. High altitude operation includes integration over larger column content that increases the optical depth, which enhances measurement sensitivity.

A new capability of the 2-μm laser was developed to produce three successive pulses. The triple-pulse IPDA lidar transmitter generates three successive laser pulses for each pump pulse. Appling the triple-pulse capability for IPDA transmitter allows simultaneous and independent measurement of CO_2 and water vapor (H_2O), the dominant interfering molecule in CO_2 measurement. On the other hand, the same capability allows measuring the CO_2 concentrations using two different weighting functions, simultaneously. Currently a 2-μm triple-pulse IPDA is under development at LaRC [8]. This triple-pulse IPDA focuses on the simultaneous and independent measurement of H_2O and CO_2 differential optical depths from an airborne platform. This system is a technological upgrade to the knowledge gathered from the 2-μm CO_2 double-pulse IPDA lidar system [15]. This paper presents the concept, development, integration and testing of the 2-μm triple-pulse IPDA.

2. TRIPLE-PULSE IPDA LIDAR TECHNIQUE

The triple-pulse IPDA lidar transmitter generates three successive laser pulses for every pump pulse. Q-switch timing, relative to the pump pulse, controls the energy distribution between the pulses. The concept of the triple-pulse IPDA is given in figure 1. The pump repetition rate is set to 50 Hz with pulse separation time of 150-200 μs, as shown in the figure. Each of the generated pulses can be tuned and locked separately to any wavelength position with respect to the R30 CO_2 absorption line. The wavelength selection of each pulse is marked on figure 2. The CO_2 on and off-line wavelengths are selected around the R30 line, so that both would have similar H_2O absorption to minimizes water vapor interference on CO_2 measurements. Similarly, H_2O on- and off-line are selected around the nearest H_2O absorption peak such that carbon dioxide interference is minimized in the H_2O measurement. However, both CO_2 on-line and H_2O off-line measurements share the same wavelength, which enables simultaneous measurement of both molecules with three pulses rather than four pulses.

Other measurements over different scenarios could be achieved with the same IPDA instrument by tuning and locking the operating wavelengths of the three pulses to different spectral positions. For example, wavelength tuning allows measuring CO_2 with two different weighting functions simultaneously as shown in figure 2. The figure indicates that the selected CO_2 on-line wavelength is optimized for near-surface measurements. Shifting this wavelength by 67 or 75 pm would tune the weighting function to optimize measurements in the boundary layer or lower troposphere. This tuning feature results in a unique adaptive targeting capability. For an airborne IPDA lidar, adaptive targeting would tune and lock the instrument sensing wavelength to meet certain measurement objective depending on the target or Earth's surface condition and environment.

3. TRIPLE-PULSE IPDA LIDAR TECHNOLOGY

The 2-μm triple-pulse IPDA lidar consists of a laser transmitter, receiver and data acquisition system. A new triple-pulse laser transmitter was developed for this IPDA. The same double-pulse receiver was used for the triple-pulse system, except an advanced HgCdTe (MCT) electron-initiated avalanche photodiode (e-APD) based detection system was placed

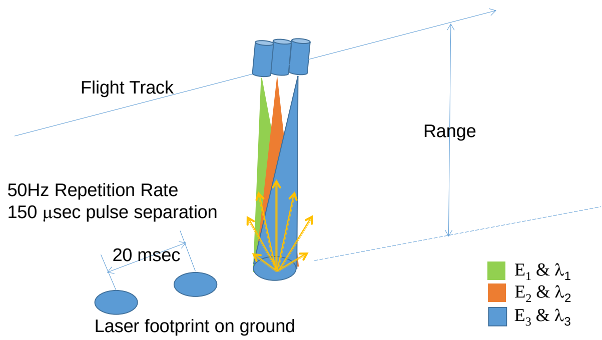

Figure 1. Airborne nadir 2-µm triple-pulse IPDA lidar concept. Each pulse is generated with different wavelength and energy. The three pulses are transmitted every 30 ms, equivalent to 50 Hz repetition rate. Pulse separation of 150-200 µs between on- and off-line results in higher than 95% laser footprint overlap from above 4 km aircraft altitude.

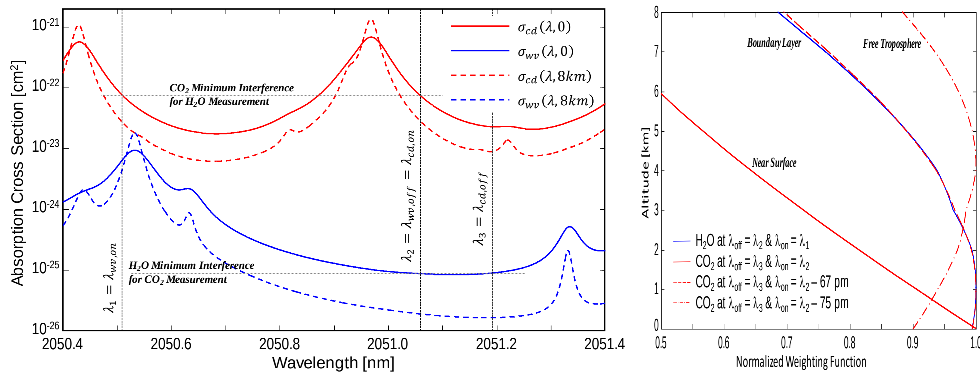

Figure 2. (Left) comparison of H_2O and CO_2 absorption cross-sections at sea-level and 8 km altitude. Vertical lines mark the instrument operating wavelengths. (Right) H_2O and CO_2 pressure-based normalized weighting functions versus altitude at the IPDA operating wavelength. Tuning CO_2 on-line 67 and 75 pm away from the selected location optimize IPDA measurement from surface to within the boundary layer or lower troposphere. Simulations conducted using the US standard atmospheric model [8].

in the low signal channel [16]. Significant data acquisition improvement was achieved by increasing the sampling rate of the waveform digitizers.

3.1 Transmitter

The triple-pulse IPDA transmitter is based on the Ho:Tm:YLF high-energy 2-µm laser technology. The laser is end pumped using 792 nm AlGaAs laser diode arrays. This external pumping targets the thulium (Tm), which transfer the energy to the holmium (Ho) relying on the different excitation lifetime. Relative to the pump pulse, Q-switch trigger produces up to three successive laser pulses with relatively controlled energies and pulse-widths. Figure 3 compares the generated output laser energies for single, double and triple-pulse operation versus the pump laser energy. Thermal analysis was conducted for proper heat dissipation out of the laser crystal to avoid permanent damage. Figure 3 also shows an oscilloscope record for a single-shot pulse. Setting the successive pulse energies to 13.3, 10.4 and 11.4 mJ result in pulse-widths of 43.7, 55.6 and 54.3 ns, respectively. A timing control unit is used to control the laser operation as well as providing timing signals to synchronize other units, such as the data acquisition system. The laser timing control unit is managed by software that set different operation parameters, such as number of pulses, wavelength of each pulse and time limits, through a graphical user interface (GUI). The wavelength of each pulse is generated using the wavelength control unit.

The objective of the wavelength control unit is to provide the required seeding for each of the generated pulses. The unit uses a single semiconductor laser diode, obtained from NASA Jet Propulsion Laboratory, and provides three different seeds of any frequency setting within 35 GHz offset from the locked CO_2 R30 line center reference [17]. This unit includes several electronic, optical and electro-optic components, which were acquired and characterized. Laser diode driver electronics result in a wavelength jitter of ±6.1 MHz. This jitter is significantly reduced to ±650.1 kHz using center line locking electronics. Figure 4 shows optical spectrum analyzer scans for the seeding wavelengths at 6, 16 and 32 GHz offset from the center line locking corresponding to the wavelength settings shown in figure 1. Proper filters are included for harmonics elimination to maintain spectral purity. Through synchronization with the pulse laser Q-switch, the wavelength switches to match the pulse event as selected by the operating software.

The 2-µm laser was populated on an optical bench that is integrated inside a laser enclosure box. The optical bench deign includes water circulation for thermal stability. Rigid optical mounts were designed and manufactured for mechanical stability. This is critical to maintain alignment during airborne operations in a vibrating environment. The laser enclosure box is hermetically sealed with purging option. The box includes electrical and fiber connections as well as an output window. The seeded 2-µm laser beam is transmitted coaxially with the receiver telescope after beam expansion. A single automated mount is used for bore-sight alignment. Energy and pulse monitors, installed inside the laser enclosure, ensure proper seeding and measure the energy of each of the transmitted pulses.

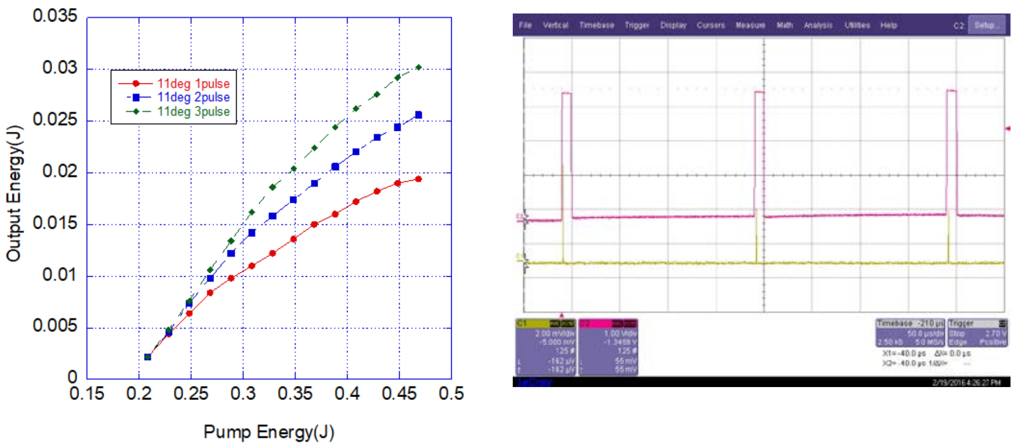

Figure 3. (Left) total output pulse energy versus pump laser energy for the 2-µm IPDA transmitter for single, double and triple-pulse operation. (Right) oscilloscope record for a the three pulses (yellow) generated using single pump pulse as compared to the Q-switch signal (red).

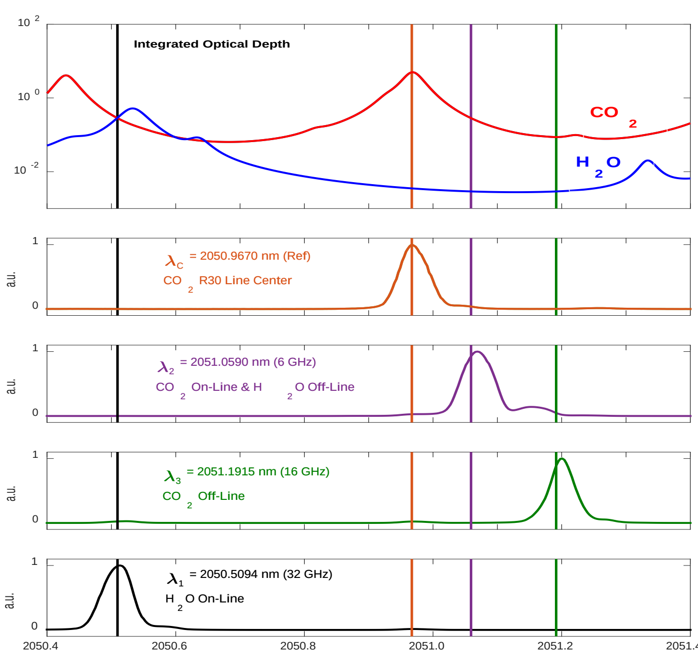

Figure 4. CO_2 and H_2O integrated optical depth spectra as compared to an optical spectrum analyzer scans for the reference locked wavelength and the three generated seeding wavelengths for the triple-pulse IPDA transmitter.

3.2 Receiver

The 2-µm triple-pulse IPDA lidar receiver is similar to the double pulse IPDA as shown schematically in figure 5. It consists of a 0.4 m Newtonian telescope that focuses the radiation onto a 300-µm diameter spot. The telescope secondary mirror is a two surfaces dichroic flat. The primary-side surface turns the return radiation 90^o to aft-optics integrated on the side of the telescope. The opposite surface is used to transmit the expanded laser beam coaxially with the telescope. The radiation collected by the telescope is focused, collimated, filtered then applied to a 90%-10% beam splitter. The 90% signal channel is an exact replica of the double-pulsed lidar using an InGaAs pin photodiode detection system. The 10% channel is coupled to the MCT e-APD detection system through an optical fiber. These e-APD devices are space-qualifiable and were validated for airborne lidar operation at 1.6-µm at NASA Goddard Space Flight Center (GSFC). In co-ordination with NASA Earth Science Technology Office (ESTO), LaRC collaborated with GSFC to integrate this detector into the 2-µm IPDA. The e-APD comes in 4 by 4 pixel format (80×80 μm^2 pixel area) with read-out electronics that enable access to each pixel through individual TIA. An output summing-amplifier would produce the sum of specific number of pixels as selected by the operator. Additional custom designed aft-optics allows focusing the radiation onto selected number of pixels. Characterization of e-APD detection system resulted in 1.4 fW/Hz$^{1/2}$ noise-equivalent- power (NEP) operating at 12 V at 77.6K [16].

3.3 Data Acquisition

The IPDA detected signals are digitized and stored using the data acquisition unit. The data acquisition unit is based on two similar high-performance digitizers (Agilent; U5303A). These digitizers are 12-bit two-channel devices that are operated at a fixed sampling rate of 1 GS/s and triggered using the laser Q-switch signal. One digitizer is dedicated to the IPDA return signals, with a variable record length of about 70k samples, while the other is dedicated to the laser energy monitors, with a fixed record length of 10k. The digitizer's data acquisition software was compiled using LabView that include GUI shown in figure 5. The software allows the operator to select the recorded data in either raw or processed formats, with raw data in either binary or MATLAB formats. The processed data are the compressed results of the displayed data that mainly include real-time background, pulse peak, pulse width, integration, energy, and UTC time for each laser shot. The digitizers are hosted in a rack-mountable computer.

4. TRIPLE-PULSE IPDA LIDAR INTEGRATION

The IPDA lidar integration includes installation, operation and optimization of the whole instrument. The integration was conducted in a mobile trailer with IPDA pointing in the nadir, which resembles orientation on the aircraft. Installation involves connecting different subsystems mechanically, optically and electrically. This includes attaching the laser enclosure box to the telescope, connecting water chillers for stabilizing the optical beanch temperature and heat sinking of thermally active components, as well as electrical and fiber optic hookups. IPDA lidar operation procedures insure system thermal and mechanical stability and successful communications and synchronization between the different units. The objective is to obtain consistent steady-state performance, in terms of timing, pulse generation and energy, without clipping or saturating IPDA signals. IPDA lidar operation procedures also insure consistent data recording and real-time processing. IPDA optimization focuses on time synchronization and optical alignments. Time

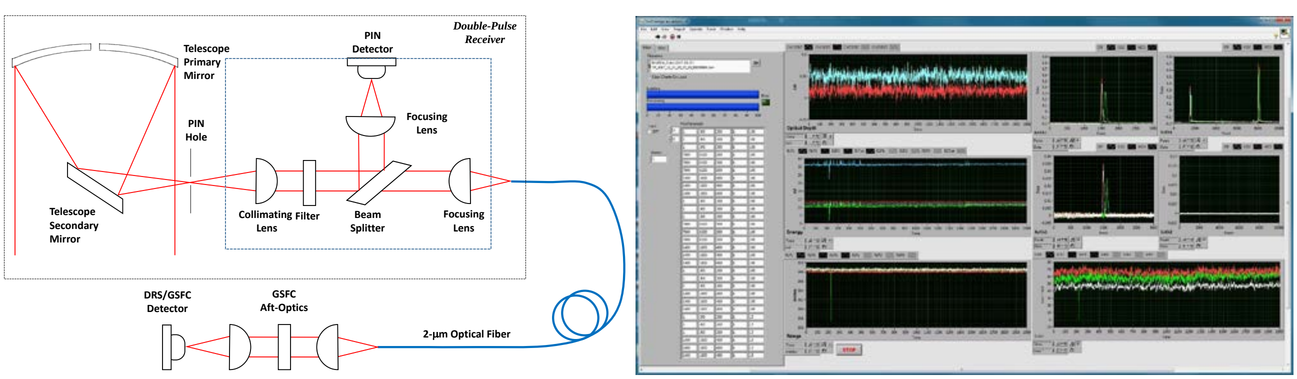

Figure 5. (Left) schematic of the triple-pulse IPDA receiver optics. The low-signal channel fiber coupled to the MCT e-APD detection system integrated at GSFC. (Right) screen shot of the data acquisition GUI used for real-time data display.

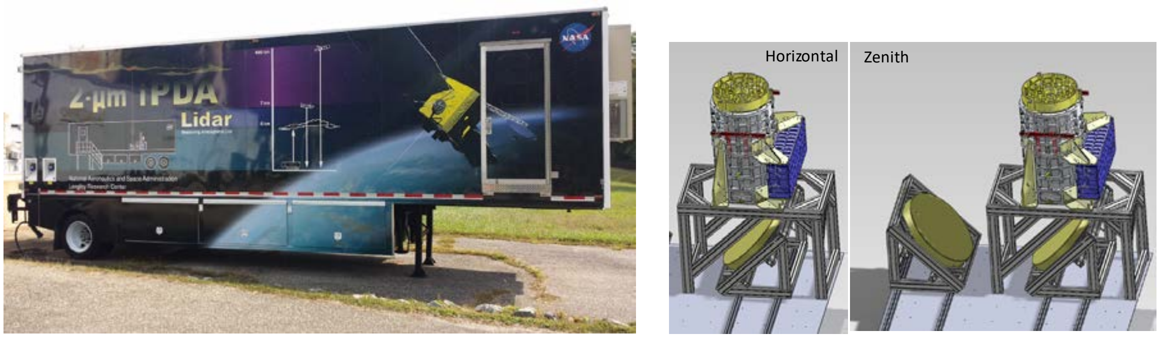

Figure 6. (Left) picture of the mobile trailer used for IPDA ground integration and testing. (Right) trailer allows IPDA horizontal or zenith pointing, through side and top windows, using turn mirrors while maintaining airborne nadir pointing.

Figure 7. Aerial picture of the IPDA ground testing site at NASA LaRC.

synchronization includes Global Positioning System (GPS) time stamp of each shot that allows synchronizing IPDA with other supporting instruments for data analysis and retrieval, and instrument modeling. IPDA supporting instruments mainly include instruments for in-situ sampling and meteorological parameters, the GPS and inertial navigation system (INS) unit during airborne operations. Optical alignment mainly focuses on optimizing IPDA return signals. This includes telescope alignment to the aft-optics, aft-optics alignment to the detectors, transmitter alignment to telescope, and during ground testing, telescope alignment to the calibrated hard target.

4.1 Trailer Integration

The IPDA lidar was integrated and installed inside a mobile trailer, shown in figure 6, for initial testing and alignment verification. The IPDA is pointing in the nadir with two 24 inch flat mirrors used in the trailer to change the instrument pointing orientation either horizontally or vertically through side and upper windows, as shown in figure 6. Horizontal pointing allows aiming the IPDA to the calibrated hard targets, with known reflectivity, located about 900 m away from the trailer. Vertical pointing allows aiming the IPDA to clouds. Figure 7 shows an aerial picture of the test site at NASA LaRC. Collocated on the site is the Chemistry and Physics Atmospheric Boundary Layer Experiment (CAPABLE). CAPABLE is a ground-based observation site that provides continuous near-surface meteorological monitoring for pressure, temperature and relative humidity among other atmospheric constituent. A CO_2 and H_2O in-situ gas analyzer (LiCor; LI-840A) was used during ground testing, for independent estimates of the gases during IPDA testing. It is worth mentioning that the trailer is collocated with the Hampton-NASA Steam Plant, which is a solid waste incinerator used for steam generation. Depending on the incinerator operating cycles, higher than normal CO_2 mixing ratio were observed at the IPDA test location.

4.2 Aircraft Integration

The design of the 2-µm triple-pulse IPDA lidar is compatible with the payload of a small research aircraft. The IPDA size, weight and power consumption were restricted to the NASA B-200 payload requirements. This allows the system to adopt to any larger airborne research platform. The aircraft integration included the IPDA transmitter/receiver structure and three racks. Table 1 lists the size, weight and power consumption for the different components and units installed in each rack. The transmitter/receiver structure consists of the telescope, laser transmitter and aft-optics boxes. The instrument control rack hosts the main units required for IPDA operation, such as the laser timing control, wavelength control and data acquisition computer. The chiller rack hosts the two chillers required for laser temperature control. The instrument support rack hosts the MCT e-APD detection system and other supporting instruments. During airborne testing an in-situ sampling instrument (PICARRO) was used to monitor CO_2 and H_2O at the aircraft location. Other supporting instruments included GPS/INS unit, and aircraft meteorological sensors. Figure 8 shows a schematic of the planned IPDA aircraft integration and pictures of the integrated instrument inside the NASA B-200.

5. TRIPLE-PULSE IPDA LIDAR TESTING

The main objective of the IPDA lidar testing is to demonstrate the instrument capability to measure two different atmospheric species, simultaneously, using a single instrument. Once this objective was achieved on ground, it was repeating in an airborne environment.

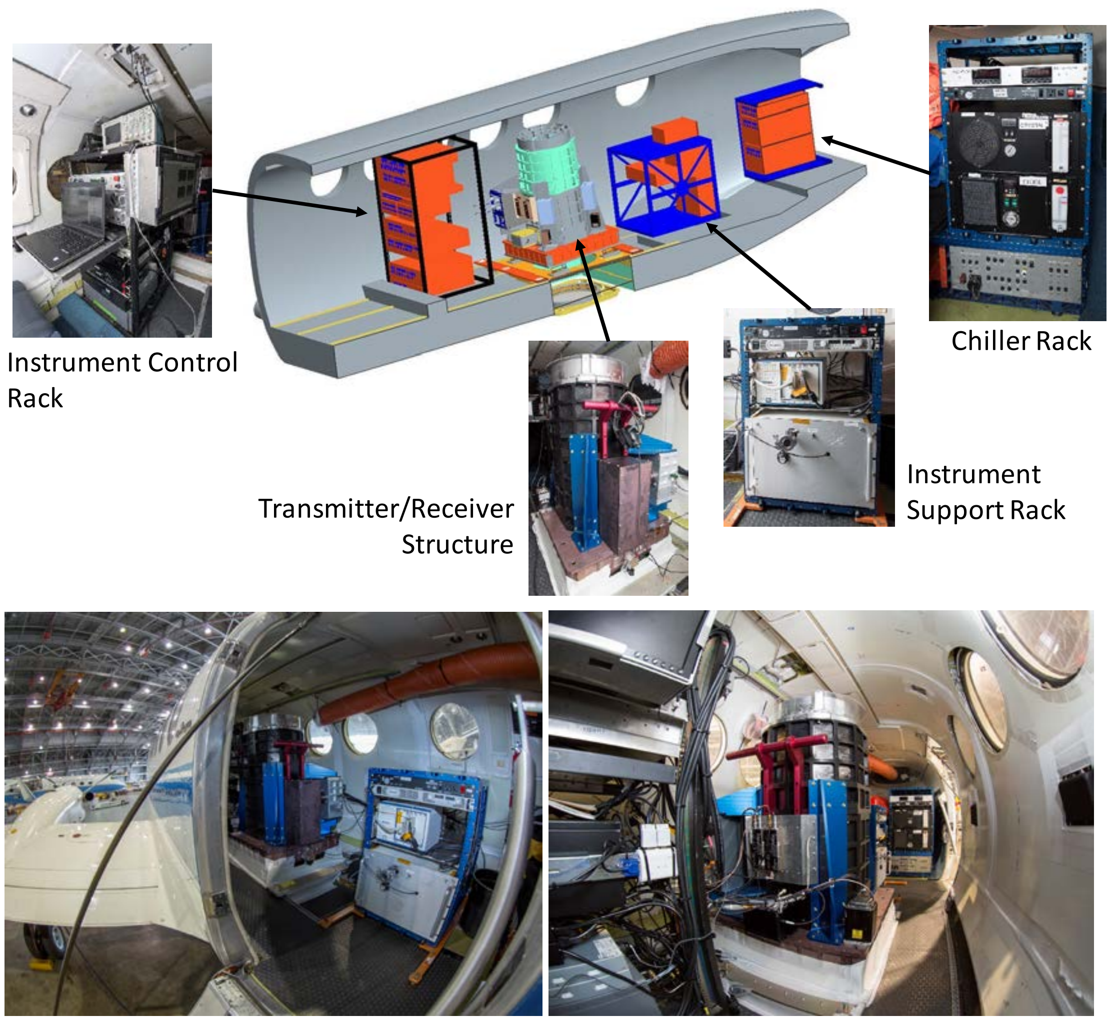

Figure 8. (Top) schematic of the planed IPDA lidar integration inside NASA B-200 aircraft and insets pictures of the actual structures. (Bottom) pictures of the integrated IPDA.

Table 1. Detailed sizes of width, height and depth; weight and power consumption of the different components of the IPDA lidar.

Unit / Component	**Size Inch^3**	**Weight lb**	**Power W**
	Transmitter/Receiver		
	24.0×30.0×16.0	208	---
	Instrument Control Rack		
Laser Diode Driver	17.3×3.5×17.0	20	240
Laser Timing Control	17.3×3.5×22.0	20	220
Wavelength Control	17.3×3.5×24.0	30	4
Oscilloscope	17.3×1.8×12.0	7	70
Data Acquisition Computer	17.3×7.1×20.0	40	
Instrument Control Laptop	17.3×1.8×20.0	5	70
Uninterrupted Power Supply	17.3×1.8×15.0	23	0
CO_2 / H_2O In-Situ Sensor	17.3×7.1×17.2		
LCD Stowable Monitor		20	20
Power-Line Filter (×2)	17.3×1.8×10.0	7	10
	Chillers Rack		
Flow Meter	17.3×1.8×11.0	5	8
Chiller 1	17.3×8.8×17.0	50	400
Chiller 2	17.3×8.8×17.0	50	375
Power-Line Filter	17.3×1.8×10.0	7	10
	Instrument Support Rack		
Extension PIXI Chase	10.1×6.9×8.5	15	60
Power Supply	19.0×1.8×17.0	20	52
MCT e-APD Detection System	19.0×12.3×24.0	75	23
Pump	5.0×6.5×7.5	22	156
Power-Line Filter	17.3x1.8x10.0	7	10

5.1 Ground Testing

The primary objective of the ground test was to ensure successful IPDA operation before aircraft integration, after integrating the various sub-systems of the instrument. Testing the IPDA operating parameters was conducted, in terms of temperatures, detection gain and bandwidth, alignments, data acquisition and long-term stability of the measurements. This was performed using different environmental and target conditions, such as calibrated hard targets reflectivity (ranging from 4 to 55%), clouds, temperatures and humidity during day and night. Figure 9 shows typical IPDA hard target return and energy monitor signals, obtained during horizontal operation using both pin and e-APD detection channels. The seeding sequence of the three pulses is 32, 6 and 16 GHz offsets from the line center. Return signal are processed by background subtraction, peak detection and pulse integration. The pulse integration was conducted to convert the return powers into energies to account for the differences in pulse widths. The primary product of the IPDA lidar is the optical depth, which is obtained by the natural logarithm of ratio of the received and transmitted off- and on-line signal energies. Other data products include ranging, pulse energies, pulse widths and return powers. Figure 10 shows a 2.5 minutes (7500 shots) sample record of the IPDA data products. These results indicate IPDA range measurement of 897 m with range uncertainty of 0.2 m. This range result is consistent with Rangefinder measurement of 894 m. IPDA range uncertainty is consistent with the digitizer's sampling rate of 1 ns, equivalent to 0.15m. A summary of the statistical analysis and comparisons with the instrument modeling are presented in Table 2. For column weighted-average dry-air mixing ratios, listed in Table 2, other ancillary data including atmospheric pressure, temperature and relative humidity, are obtained from CAPABLE site. Figure 11 shows typical IPDA signals obtained through vertical operation by targeting both low altitude cumulus and high altitude cirrus clouds using the e-APD detection channel.

5.2 Airborne Testing

The IPDA lidar was tested during four flights (over 20 hours) conducted to achieve various goals. Figure 12 shows the GPS tracks of the flights. Each flights included two IPDA operators. The first flight was to verify instrument operation and performance using different settings at the highest altitude. The second flight was conducted over ocean targeting clear, broken cloud and cloudy conditions. Meteorological balloon radiosonde was independently lunched from LaRC to validate the aircraft metrological sensors during down-spiral maneuver. The third flight was coordinated with

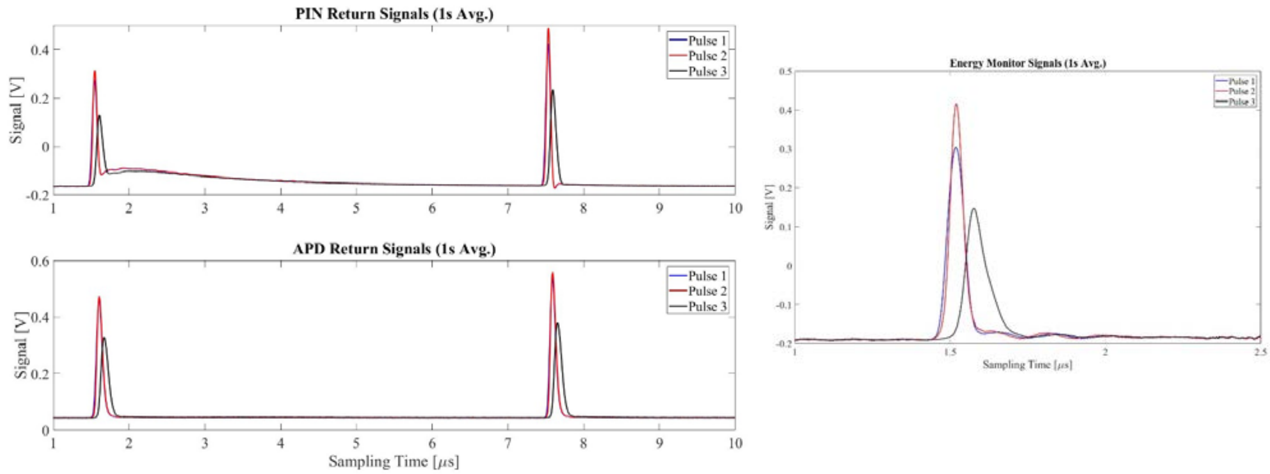

Figure 9. Triple-pulse, 2-μm IPDA typical hard target return, using pin (top, left) and e-APD (bottom, left) detection systems, and energy monitor signals (right). IPDA was pointed horizontally at the 4% reflectivity target. Seeding sequence of 32, 6, and 16 GHz for pulses 1, 2 and 3, respectively. Signals are averaged over 50 shots (1-s), with PIN TIA gain setting of 104 V/A, and e-APD was set to a single pixel (#10) using 2.5 V.

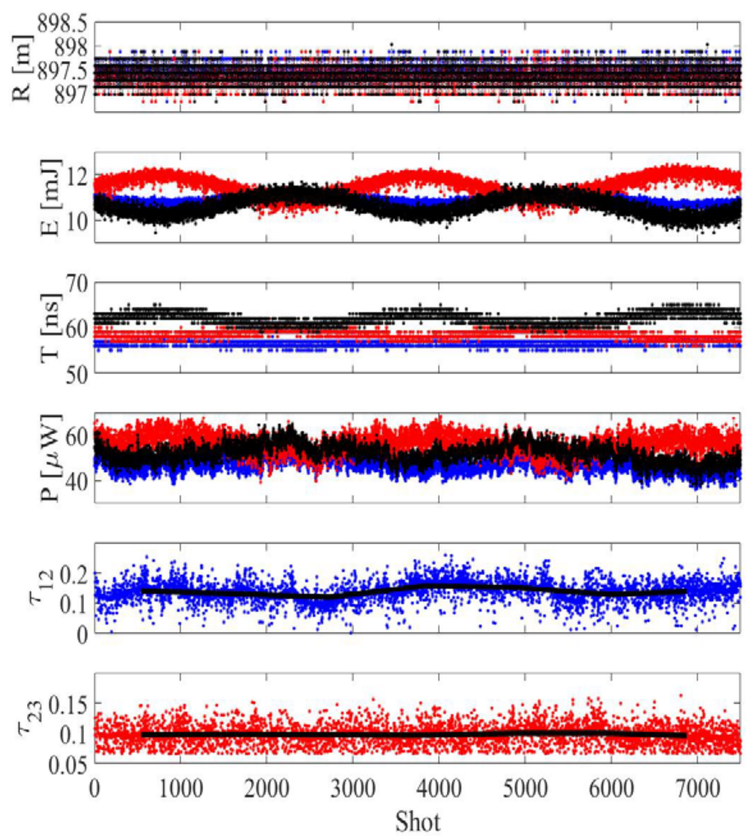

Figure 10. Triple-pulse, 2-μm IPDA ground testing data products including, range (R), pulse energies (E), return pulse widths (T), return powers (P), and H_2O and CO_2 optical depths (τ_{12} and τ_{23}, respectively). Single-shot data are presented for pin detection channel for 2.5 minute records (7500 shots), with 32, 6, 16 GHz seeding. This IPDA testing was conducted on January 10, 2018. Results are compared to instrument simulations conducted using US standard atmospheric model and meteorological data using CAPABLE and in-situ measurements, as listed in Table 2. Blue, red, and black points represent the first, second and third pulse data, respectively in top four plots. Dots represent per-shot data and sloid black curves represents 10-s averaged data for the two bottom plots.

Table 2. Statistical analysis of the triple-pulse 2-μm IPDA lidar simultaneous and independent measurements of CO_2 and H_2O, presented during ground (figure 10) and airborne (figure 12) testing. Results are compared to instrument simulations using meteorological data and US standard atmosphere. CO_2 profile of the US standard atmosphere was updated using 422 ppm surface value.

	CO_2	H_2O
Differential Optical Depth Measurements, Ground Testing		
Single-Shot	0.0955 ± 0.0215	0.1408 ± 0.0361
50 Shots Average (1 s)	0.0986 ± 0.0049	0.1384 ± 0.0182
500 Shots Average (10 s)	0.0987 ± 0.0015	0.1382 ± 0.0134
Meteorological Model	0.1045 ± 0.0001	0.1759 ± 0.0005
US Standard Atmospheric Model	0.1029	0.1866
Weighted-Average Column Dry-Air Volume Mixing Ratio Retrievals [in ppm], Ground Testing		
Single-Shot	392.3 ± 71.9	5057.8 ± 1398.8
50 Shots Average (1 s)	436.9 ± 19.8	5037.1 ± 673.2
500 Shots Average (10 s)	425.9 ± 6.0	5353.2 ± 496.6
Meteorological Model	422.0 ± 0.4	6481.9 ± 17.5
US Standard Atmospheric Model	422.0	7750.0
Differential Optical Depth Measurements, Airborne Testing		
Single-Shot	0.3692 ± 0.1609	0.1709 ± 0.2124
50 Shots Average (1 s)	0.3724 ± 0.0224	0.1840 ± 0.0284
500 Shots Average (10 s)	0.3704 ± 0.0079	0.1864 ± 0.0124
US Standard Atmospheric Model	0.3895	0.5623

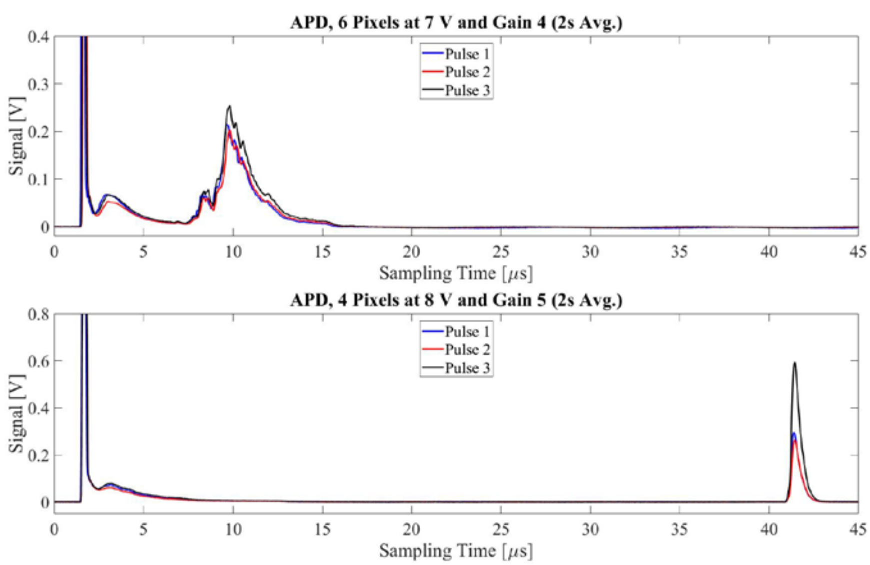

Figure 11. Triple-pulse, 2-μm IPDA typical clouds return, using e-APD detection system. IPDA was pointed vertically (zenith) targeting 1.2 km altitude cumulus clouds (top) and 6 km cirrus clouds (bottom). The seeding sequence is 32, 6, and 16 GHz for pulse 1, 2 and 3, respectively. Signals are averaged over 100 shots (2-s), with e-APD cooled to 77 K, with the listed active number of pixels and biases.

NOAA and university of Maryland for comparison of the IPDA results and on-board in-situ sensor measurements with other, independently operated, CO_2 air sampling and in-situ sensor data. IPDA on-board NASA B-200 flew over the ocean off Cape May, NJ, at nine different altitudes, following the NOAA's aircraft. Then, the B-200 flew over land, north-east of Baltimore, MD, at 5 km altitude to capture urban plums with NIST calibrated CO2 sensor on-board another aircraft, at 2.5 km altitude, operated by University of Maryland. The fourth flight was conducted over Roxboro Power Station (Semora, NC), at different altitudes during day and night for plum detection. The instrument performance met the design objectives, demonstrating the measurements of two atmospheric specie simultaneously and independently from an airborne platform. Figure 13 shows a 1 minute (3900 shots) sample record of the IPDA data products, obtained from 7.7 km altitude flying off the coast of Cape May, NJ. Table 2 lists a summary of airborne data sample, shown in the figure.

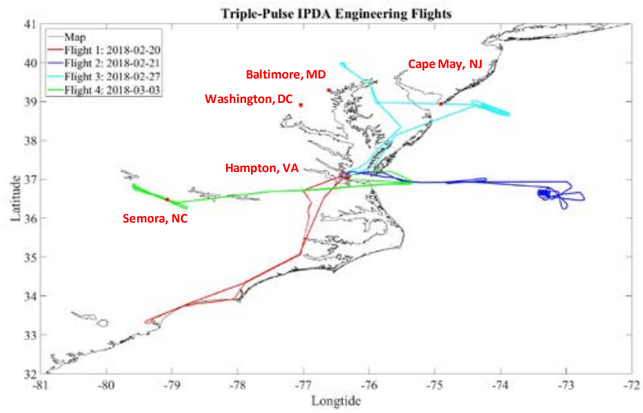

Figure 12. Triple-pulse 2-μm IPDA GPS flight track records for the four flights conducted for instrument airborne testing.

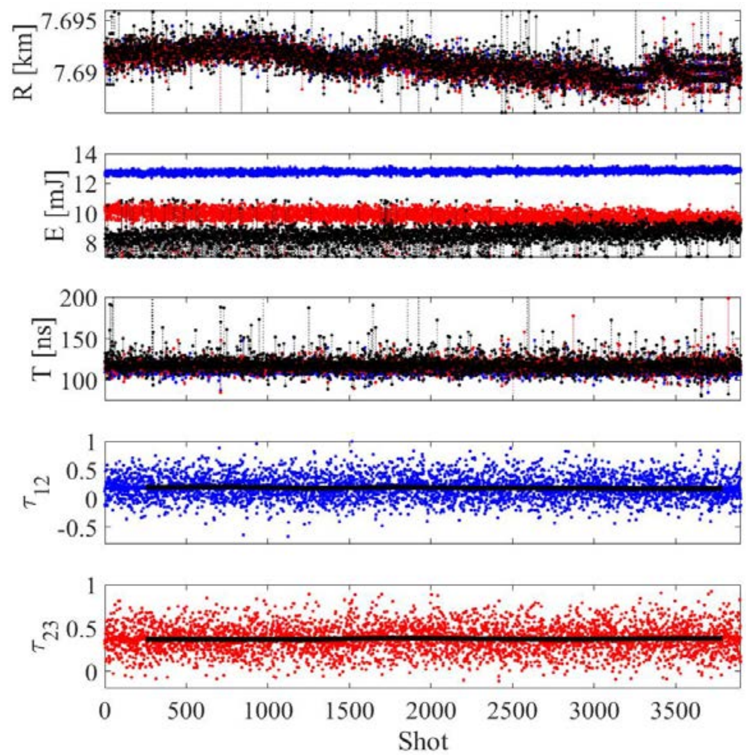

Figure 13. Triple-pulse, 2-μm IPDA airborne data products including, range (R), pulse energies (E), return pulse widths (T), and H_2O and CO_2 optical depths (τ_{12} and τ_{23}, respectively). Single-shot data are presented for pin detection channel for 1 min. record (3900 shots), with 32, 6, 16 GHz seeding. This IPDA testing was conducted on February 27, 2018, over ocean at Cape May onboard NASA B-200 aircraft. Blue, red, and black points represent the first, second and third pulse data, respectively in top three plots. Dots represent per-shot data and sloid black curves represents 10-s averaged data for the two bottom plots.

6. CONCLUSION

NASA LaRC successfully demonstrated an airborne tripled-pulsed 2-μm IPDA lidar for simultaneous and independent measurements of atmospheric carbon dioxide and water vapor – a unique active remote sensing capability. IPDA transmitter delivers, high-energy, three pulses at three different locked wavelengths at 50 Hz, with 200 μs pulse separation. The instrument design was based on the successful demonstration of the double-pulse IPDA lidar for carbon dioxide measurements. Instrument development and integration was successfully accomplished. Ground and airborne testing indicated successful operation of the IPDA instrument. Airborne testing was conducted over land, ocean, vegetation and plumes from power plant. Coordinated flights were conducted with NOAA and NIST/University of Maryland over New Jersey Bay and Washington/Baltimore urban areas. In preparation for the next science validation, which is planned at the end of 2018, the IPDA lidar is currently operated in a mobile trailer and its performance is being assessed and required improvements and updated will be made.

ACKNOWLEDGMENT

The authors would like to acknowledge NASA Earth Science Technology Office for supporting this work.

REFERENCES

[1] T. Refaat, S. Ismail, G. Koch, M. Rubio, T. Mack, A. Notari, J. Collins, J. Lewis, R. DeYoung, Y. Choi, N. Abedin, and U. Singh, "Backscatter 2-μm lidar validation for atmospheric CO_2 differential absorption lidar applications," IEEE Trans. on Geosc. and Remote Sensing, 49(1), 572 (2011).

[2] T. Refaat, S. Ismail, G. Koch, L. Diaz, K. Davis, M. Rubio, N. Abedin, and U. Singh, "Field testing of a two-micron DIAL system for profiling atmospheric carbon dioxide," 25^{th} Int. Laser Radar Conf., St. Petersburg, Russia (2010).

[3] G. Koch, J. Beyon, F. Gibert, B. Barnes, S. Ismail, M. Petros, P. Petzar, J. Yu, E. Modlin, K. Davis, and U. Singh, "Side-line tunable laser transmitter for differential absorption lidar measurements of CO_2: design and application to atmospheric measurements," Appl. Opt., 47(7), 944 (2008).

[4] T. Refaat, U. Singh, J. Yu, M. Petros, R. Remus, and S. Ismail, "Double-pulse 2-μm integrated path differential absorption lidar airborne validation for atmospheric carbon dioxide measurement," Appl. Opt., 55(15), 4232 (2016).

[5] T. Refaat, U. Singh, M. Petros, R. Remus, and J. Yu, "Self-calibration and laser energy monitor validations for a double-pulsed 2-μm CO2 integrated path differential absorption lidar application," Appl. Opt., 54(24), 7240 (2015).

[6] T. Refaat, U. Singh, J. Yu, M. Petros, R. Remus, and S. Ismail, "Airborne two-micron double-pulse IPDA lidar validation for carbon dioxide measurements over land," 28^{th} Int. Laser Radar Conf., Bucharest, Romania (2017).

[7] U. Singh, J. Yu, M. Petros, T. Refaat, R. Remus, J. Fay and K. Reithmaier, "Airborne 2-micron double-pulsed integrated path differential absorption lidar for column CO_2 measurement," Proc. SPIE, 9246, 924602 (2014).

[8] T. Refaat, U. Singh, J. Yu, M. Petros, S. Ismail, M. Kavaya, and K. Davis, "Evaluation of an airborne triple-pulsed 2 μm IPDA lidar for simultaneous and independent atmospheric water vapor and carbon dioxide measurements," Appl. Opt., 54(6), 1387 (2015).

[9] U. Singh, M. Petros, T. Refaat, and J. Yu, "2-micron triple-pulse integrated path differential absorption lidar development for simultaneous airborne column measurements of carbon dioxide and water vapor in the atmosphere," Proc. SPIE, 9879, 987902 (2016).

[10] U. Singh. T. Refaat, S. Ismail, K. Davis, S. Kawa, R. Menzies, and M. Petros, "Feasibility study of a space-based high pulse energy 2 μm CO_2 IPDA lidar," Appl. Opt., 56(23), 6531 (2017).

[11] J. Yu, M. Petros, U. Singh. T. Refaat, K. Reithmaier, R. Remus, and W. Johnson, "An airborne 2-μm double-pulsed direct-detection lidar instrument for atmospheric CO_2 column measurements," J. of Atmos. and Ocea. Tech., 34, 385 (2017).

[12] U. Singh, B. Walsh, J. Yu, M. Petros, M. Kavaya, T. Refaat, and N. Barnes, "Twenty years of Tm:Ho:YLF and LuLiF laser development for global wind and carbon dioxide active remote sensing," Opt. Mate. Express, 5(4), 827 (2015).

[13] T. Refaat, M. Petros, C. Antill, U. Singh and J. Yu, "Wavelength locking to CO_2 absorption line-center for 2-μm pulsed IPDA lidar application," Proc. SPIE, 9879, 987904 (2016).

[14] J. Yu, B. C. Trieu, E. A. Modlin, U. N. Singh, M. J. Kavaya, S. Chen, Y. Bai, P. J. Petzar, and M. Petros, "1 J/pulse Q-switched 2 μm solid-state laser," Opt. Lett. 31(4), 462 (2006).

[15] U. Singh, J. Yu, M. Petros, T. Refaat, R. Remus, and K. Reithmaier, "Development of double- and triple-pulsed 2-micron IPDA lidars for column CO_2 measurements," Proc. SPIE, 9612, 961204 (2015).

[16] X. Sun, J. Abshire, J. Beck, P. Mitra, K. Reiff, and G. Yang, "HgCdTe avalanche photodiode detectors for airborne and spaceborne lidar at infrared wavelengths," Opt. Exp. 25(14) 16589 (2017).

[17] M. Bagheri, G. Spiers, C. Frez, S. Forouhar, and F. Aflatouni, "Linewidth measurement of distributed-feedback semiconductor lasers operating near 2.05 μm," IEEE Photon. Technol. Lett. 27(18), 1934 (2015).